Princeton Plasma Physics Laboratory **NSTX Experimental Proposal**			
Title: **Dependence of P_{LH} on Radius of the X-point**			
OP-XP-1029	Revision:	Effective Date: *(Approval date unless otherwise stipulated)* Expiration Date: *(2 yrs. unless otherwise stipulated)*	
PROPOSAL APPROVALS			
Responsible Author: R. Maingi			Date **June 10, 2010**
ATI – ET Group Leader: H. Yuh			Date
RLM - Run Coordinator: E.D. Fredrickson			Date
Responsible Division: Experimental Research Operations			
RESTRICTIONS or MINOR MODIFICATIONS (Approved by Experimental Research Operations)			

1. Overview of planned experiment

The goal of this XP is to measure the dependence of the L-H power threshold (PLH) on the radius of the X-point, i.e. in essence a triangularity scan. Specifically we will follow-up on XP 909, trying to confirm the previous results in discharges with low dW/dt.

2. Theoretical/ empirical justification

Code calculations from XGC-0 have shown that the thermal ion loss at the X-point increases with the X-point radius, leading to the predicted formation of a larger radial electric field, E_r ,and shear, E_r'. Operating from a premise that a critical E_r or E_r'might be needed for H-mode access, it follows that discharges with large X-point radii (i.e. reduced lower triangularity δ_L) would have a lower L-H power threshold than discharges with a higher δ_L.

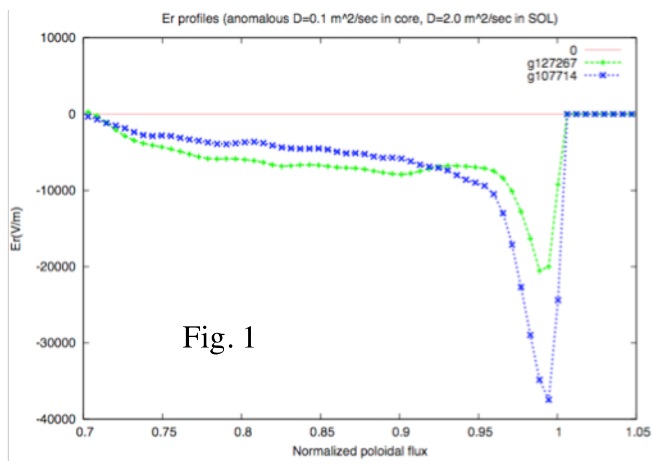

Fig. 1

Figure 1 shows a comparison of the computed E_r from the XGC-O code for a low (blue) and high δ_L (green) discharges, using the EFIT02 pressure profiles as a starting point. I can be seen that the E_r and E_r' are substantially higher for the low δ_L discharge, as previously presented by C.S. Chang.

The role of the X-point in setting PLH was investigated in XP909, and published in [R. Maingi, et. al., *Nucl. Fusion* **50** (2010) 064010]. While the raw input power was 50-60% higher for high δ discharges (Figure 2), those discharges also had the largest dW/dt terms. Hence a clear statement could not be made on the dependence of PLH (as measured by P_{loss}) on δ. Here we propose to re-run the low and high δ discharges, taking care to obtain comparable discharges with similar P_{OH} and dW/dt.

3. Experimental run plan (1/2 day)

- Develop baseline 0.8 MA, 0.45 T low and high δ discharges (based on pre-li 132721 and 132717 respectively – see Figure 3) with low levels of lithium, i.e. 50-100 mg between discharges. If ohmic H-modes are observed, 1) drop I_p to 0.7MA, 2) raise B_t to 0.5 T, 3) raise gas puff rate until they are suppressed. The goal is to obtain a relative measurement difference at low and high δ. (8)
- Delay NBI heating till after flattop for low δ discharge and measure P_{LH}. NBI started at ~ 180ms in target discharges, delay to between 200-240 ms. (6)
- Run the same NBI program for high δ discharge (1)
- Add extra NBI power 50ms after lower power level, i.e. starting at 250-290ms (5)

- Re-run low δ discharge just above P_{LH} for reproducibility check (2)
- Time permitting: re-develop and measure P_{LH} in medium δ discharge (e.g. 132708) (8)

4. Required machine, NBI, RF, CHI and diagnostic capabilities

NBI up to 6 MW, but with the ability to change voltages between shots, no CHI or rf.

5. Planned analysis

The discharges will be analyzed with TRANSP to obtain P_{loss}. The edge profiles will be analyzed with XGC-0 to determine the E_r in the L-mode phase prior to the L-H transition.

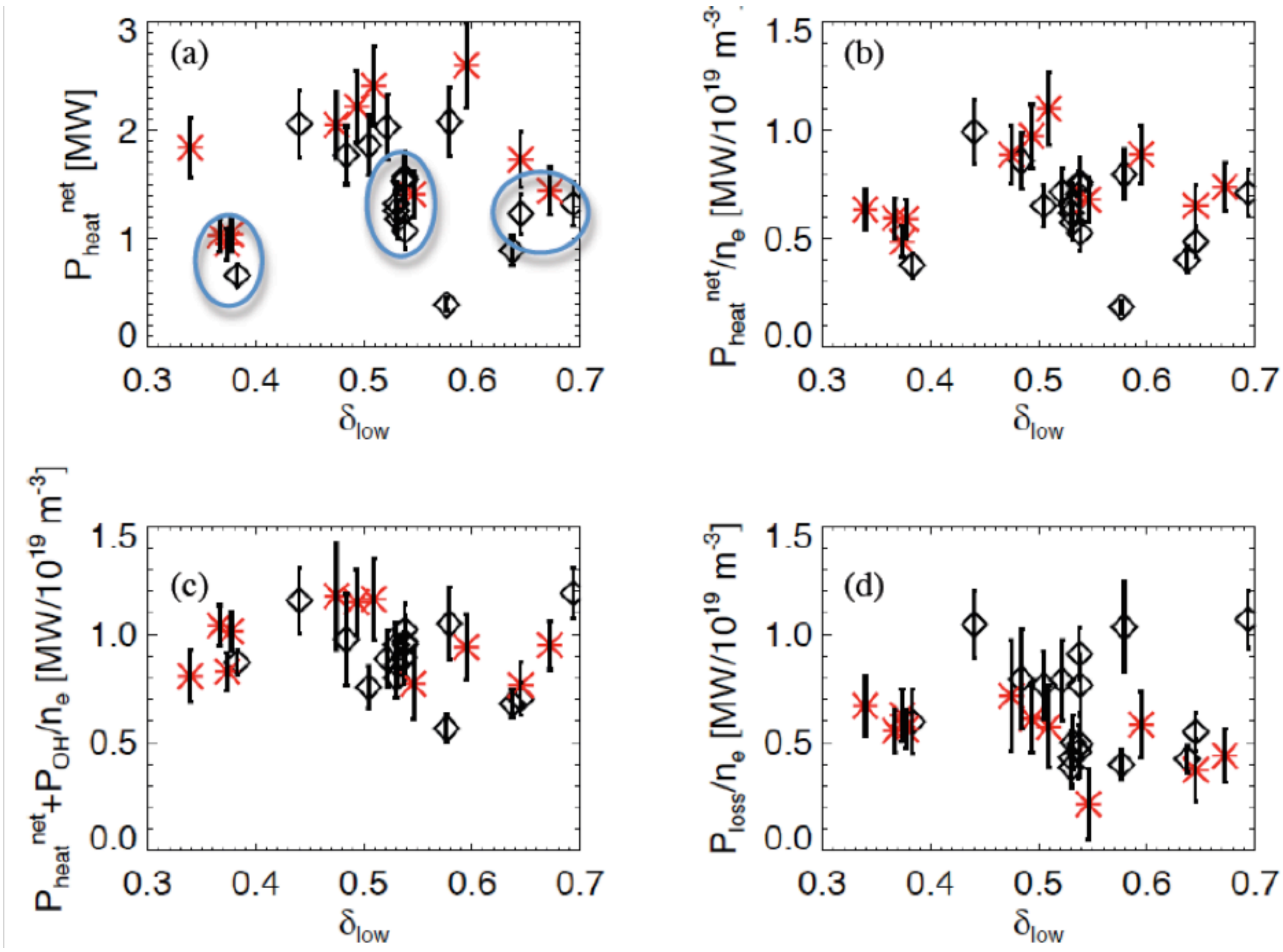

Fig. 2: Various metrics of input power as a function of lower divertor triangularity δ_{low} with NBI heating: (a) P_{heat}, (b) P_{heat} normalized by $\overline{n}_e$, (c) (P_{heat} + P_{oh}) normalized by $\overline{n}_e$, and (d) P_{loss} normalized by $\overline{n}_e$. The red stars represent data just prior to an L-H transition, and the black diamonds represent data that did not have an L-H transition. Ovals mark discharges closest to the power threshold.

6. Planned publication of results

The results will be published in a short letter in Nucl. Fusion. They will also contribute to an IAEA paper.

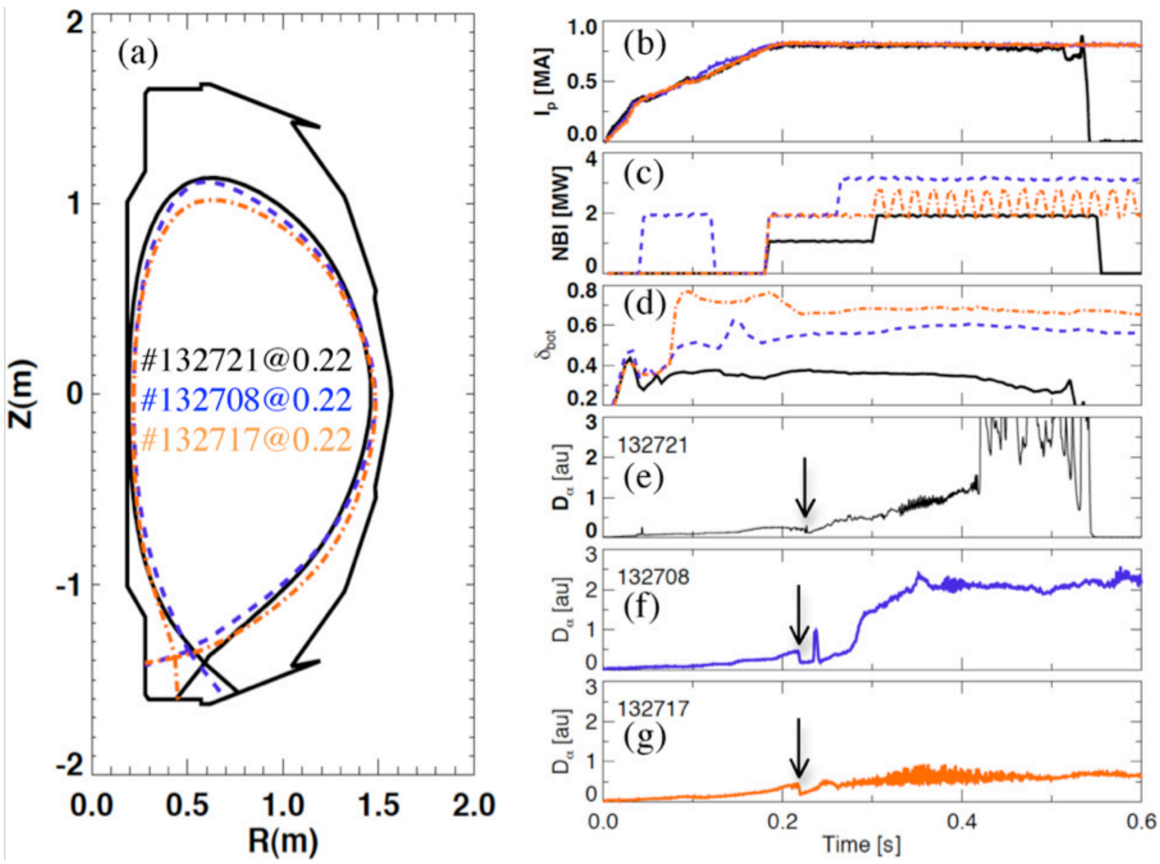

Fig. 3: Three different X-point radii (d) were developed previously in XP909.

PHYSICS OPERATIONS REQUEST

TITLE: **Dependence of P_{LH} on Radius of the X-point** No. **OP-XP-1029**
AUTHORS: **R. Maingi, S.M. Kaye, D.J. Battaglia** DATE: **June 10, 2010**

(use additional sheets and attach waveform diagrams if necessary)

Brief description of the most important operational plasma conditions required:

X-point/triangularity scan at constant X-point height at time of LH, as in previous discharges. Ohmic H-modes should be avoided.

Previous shot(s) which can be repeated:

Previous shot(s) which can be modified: 132721, 132708, 132717

Machine conditions *(specify ranges as appropriate, strike out inapplicable cases)*

I_{TF} (kA): **0.45 T** Flattop start/stop (s):

I_P (MA): **0.8 MA** Flattop start/stop (s):

Configuration: Limiter / DN / **LSN /** USN

Equilibrium Control: Outer gap / **Isoflux (rtEFIT)** / Strike-point control (rtEFIT)

Outer gap (m): **10cm** Inner gap (m): **varies** Z position (m): **varies**

Elongation: **2.0** Triangularity (U/L): **0.3-0.7** OSP radius (m): **40cm, 80cm**

Gas Species: **D_2** Injector(s):

NBI Species: **D** Voltage (kV) **A: 90** **B: 60-90** **C: 60-90** Duration (s):

ICRF Power (MW): Phase between straps (°): Duration (s):

CHI: **Off** / On Bank capacitance (mF):

LITERs: Off / **On** Total deposition rate (mg/min):

LLD: Temperature (°C): **unheated**

EFC coils: Off/**On** Configuration: **Odd** / Even / Other *(attach detailed sheet)*

DIAGNOSTIC CHECKLIST

TITLE: **Dependence of PLH on Radius of the X-point** No. **OP-XP-1029**

AUTHORS: **R. Maingi, S.M. Kaye, D.J. Battaglia** DATE: **June 6, 2010**

Note special diagnostic requirements in Sec. 4

Diagnostic	**Need**	**Want**
Beam Emission Spectroscopy		√
Bolometer – divertor		√
Bolometer – midplane array	√	
CHERS – poloidal		√
CHERS – toroidal	√	
Dust detector		
Edge deposition monitors		√
Edge neutral density diag.		√
Edge pressure gauges	√	
Edge rotation diagnostic		√
Fast cameras – divertor/LLD		√
Fast ion D_alpha - FIDA		
Fast lost ion probes - IFLIP		
Fast lost ion probes - SFLIP		
Filterscopes	√	
FIReTIP		√
Gas puff imaging – divertor		√
Gas puff imaging – midplane		√
Hα camera - 1D		√
High-k scattering		
Infrared cameras		√
Interferometer - 1 mm		
Langmuir probes – divertor		√
Langmuir probes – LLD		√
Langmuir probes – bias tile		
Langmuir probes – RF ant.		
Magnetics – B coils	√	
Magnetics – Diamagnetism	√	
Magnetics – Flux loops	√	
Magnetics – Locked modes	√	
Magnetics – Rogowski coils	√	
Magnetics – Halo currents		√
Magnetics – RWM sensors		√
Mirnov coils – high f.		√
Mirnov coils – poloidal array		
Mirnov coils – toroidal array		√
Mirnov coils – 3-axis proto.		

Note special diagnostic requirements in Sec. 4

Diagnostic	**Need**	**Want**
MSE		√
NPA – E‖B scanning		
NPA – solid state		
Neutron detectors		√
Plasma TV		√
Reflectometer – 65GHz		√
Reflectometer – correlation		√
Reflectometer – FM/CW		
Reflectometer – fixed f		
Reflectometer – SOL		√
RF edge probes		
Spectrometer – divertor		
Spectrometer – SPRED		√
Spectrometer – VIPS		
Spectrometer – LOWEUS		
Spectrometer – XEUS		
SWIFT – 2D flow		
Thomson scattering	√	
Ultrasoft X-ray – pol. arrays		√
Ultrasoft X-rays – bicolor		√
Ultrasoft X-rays – TG spectr.		√
Visible bremsstrahlung det.		√
X-ray crystal spectrom. - H		
X-ray crystal spectrom. - V		
X-ray tang. pinhole camera		